

Spectral Finite Element Method for solving Steady and Unsteady Heat Diffusion Problem

*A Project Report submitted in Partial Fulfillment
of the Requirements for the Degree of*

Master of Technology

by

Aamir Haider

234103402

Under the guidance of

Dr. Atanu Banerjee



**Department of Mechanical Engineering
Indian Institute of Technology Guwahati
November 2024**

Acknowledgement

I would like to express my sincere gratitude to my supervisor Dr. Atanu Banerjee, Department of Mechanical Engineering, IIT Guwahati, India. He was always cordial and supportive throughout the highs and lows during the period of project. He has invested a lot of time, given valuable inputs, and took great pain to see me through. I have learned a lot from him and humbly acknowledge a lifetime of deep gratitude towards him. Without his support and encouragement, this project would not have been possible.

I am deeply indebted to my parents for their unconditional love, and support. Without their teachings and blessings, I could not have come to this stage of life.

I am also thankful to my seniors Mr. Umesh Mishra, Mr. Tejdeep and all my dear friends from IITG for helping me directly or indirectly and making my life more enjoyable. Last but not least, I thank the Ministry of Human Resource Development, the government and the people of India without whom the running of this institute and thereby my Master's program is not possible.

Mr. Aamir Haider
Department of Mechanical Engineering,
Indian Institute of Technology Guwahati,
Guwahati, Assam, India, 781039,
November 2024.

Abstract

The application and use of the spectral element approach in solid and fluid mechanics are the main topics of this study. The three conventional lower order methods—the finite difference technique, the finite volume method, and the finite element approach—were used in the majority of numerical research for system analysis. These approaches’ primary drawback is their high computational cost. Simple geometries and homogenous boundary conditions are the only limitations of spectral approaches, which are the fastest approach for a given precision in computational studies. Thus, for this thesis work, the spectral element method is used.

An extension of the finite element approach, the spectral element method employs higher order polynomials, such as the spectral methods, to provide a higher order of accuracy with less computational time and the ability to handle complicated geometry. This report explains how the spectral element method compares to other numerical techniques and provides evidence for using it. After reviewing earlier studies that used the spectral element technique, gaps in the literature were noted. This approach has been widely utilized in fractional partial differential equation modeling and structural analysis because to its excellent accuracy; nevertheless, fluid-structure interaction has not benefited as much from its application. The computational expense and the use of intricate and dynamic geometries are the causes.

A lobatto based spectral element code was developed to solve problems numerically and investigate their behaviour. The results for steady and unsteady heat diffusion problem was validated with the analytical results to check the correctness of the solver. It gave a close approximation of the result with fewer degrees of freedom.

Contents

1	Introduction	1
1.1	Spectral element method	1
1.2	Elastodynamic problem	2
1.2.1	Aeroelastic Effects and Flutter Prediction	2
1.2.2	Flow Separation and Reattachment Analysis	2
1.2.3	Unsteady Aerodynamics	2
1.2.4	Aerofoil Shape Optimization	3
1.3	Fluid-Structure Interactions	3
1.4	Numerical Techniques	4
1.4.1	Finite Difference Method	5
1.4.2	Finite Volume Method	5
1.4.3	Finite Element Method	6
1.4.4	Spectral Method	6
1.4.5	Spectral Element Method	6
1.5	Literature review	7
1.5.1	Development of SEM	7
1.5.2	Spectral element method	7
1.5.3	Chebyshev spectral element method	8
1.5.4	Legendre spectral element method(LSEM)	9
1.5.5	Spectral Element-Fourier Method	9
1.6	Objectives	10
1.7	Structure of Thesis	10
2	Methodology	12
2.1	Overview of SEM	12
2.2	Galerkin Weak Formulation	13
2.3	Formulation of linear algebraic system	14
2.4	Element Level Transformation	15
2.5	Interpolation	16
2.5.1	Nodal Interpolation	16
2.5.2	Lagrange Polynomials	16

2.5.3	Lobatto polynomials	17
2.6	Steady Heat Diffusion in One Dimension	19
2.6.1	Results	20
2.7	Unsteady Heat Diffusion in One Dimension	23
2.7.1	Galerkin weak formulation	25
2.7.2	Results	27
3	Summary	28
3.1	Future Work	29
	Bibliography	29

List of Figures

1.1	Fluid-structure interaction system	4
1.2	Classification fluid-induced vibration [1]	4
1.3	Mesh based numerical techniques to solve partial differential equation [2]	5
1.4	Basics of FEM	6
2.1	SEM flowchart	12
2.2	Body-aligned mesh for case that the Orthogonality of ϵ	13
2.3	Transformation in 1D	15
2.4	Legendre and Lobatto polynomial	17
2.5	Lobatto roots and weights	17
2.6	Node location for Lobatto points	18
2.7	Interpolation of Runge's function	18
2.8	Conduction through a rod extending from $x=0$ to $x=L$ at steady state.	19
2.9	Finite element solution of steady diffusion equation with 16 linear elements with parameters $L=1.0, k=1.0, q_0=-1.0, f(L)=0.0, s_0=10.0$	21
2.10	Error for left end value for the model problem.	23
2.12	Conduction through a rod extending from $x = 0$ to $x = L$ at steady state.	24
2.13	Solution to unsteady diffusion equation by implementing the Crank-Nicolson method	27

List of Tables

2.1	Accuracy and convergence of the spectral element method compared to the finite element method.	22
-----	---	----

Chapter 1

Introduction

1.1 Spectral element method

Significant advancements in computational techniques used in research and engineering have been made in recent decades as a result of the quick advancements in computer technology. As one of the most practical and user-friendly computational techniques, the classical finite element method (FEM) has most likely been the most widely used in many branches of science and engineering. Despite being suitable to the majority of geometries, boundary conditions, and material changes, the FEM may be very costly, and solving large-scale finite element models on a desktop computer is frequently not feasible. Therefore, even today, an alternate approach that may yield precise results while lessening the computing load while maintaining the main benefits of FEM is required.

The finite element equation is formulated in the time domain and solved using a numerical integration approach in the FEM, a time-domain solution technique. In contrast, high-degree piecewise polynomials are used as basis functions in the spectral element method (SEM), which is a version of the finite element method (FEM). One of the main benefits of the spectral method is that it produces a very high order solution by expanding the answer in trigonometric series. This method is based on the observation that a space of square-integrable functions on the domain Ω has an orthonormal basis in trigonometric polynomials.

The spectral element method chooses instead a high degree piecewise polynomial basis functions, also achieving a very high order of accuracy. Such polynomials are usually orthogonal Chebyshev polynomials or very high order Lagrange polynomials over non-uniformly spaced nodes resulting in computational error decreases exponentially as the order of approximating polynomial increases.

1.2 Elastodynamic problem

The elastodynamic problem is a classical problem in the field of mechanics that deals with the study of elastic structures subjected to dynamic (time-varying) forces. It specifically entails examining the deformation and response of elastic bodies—such as beams, plates, shells, or other structures—to dynamic loads or excitations that change over time. They appear when the fluid (air) and the structure (such as a wing or aerofoil) interact to produce dynamic behavior and the structure deforms in reaction to aerodynamic forces. The following are the pertinent elastodynamic issues with aerofoils:

1.2.1 Aeroelastic Effects and Flutter Prediction

It entails the interplay between the elastic response of the structure (such as an aerofoil or wing) and the aerodynamic forces (from the wind). The aerodynamic forces are impacted by the deformations that the aerofoil undergoes as a result of the aerodynamic loads. Flutter, a self-excited oscillation that can harm or destabilize the structure, can occur under specific circumstances, making the system unstable.

The structural dynamics of the aerofoil or wing (modeled by equations of motion for deformable bodies) are coupled with the fluid dynamics (described by the Navier-Stokes equations or potential flow equations). Both the fluid flow and the structural motion equations must be solved in order to take into account the aerofoil's elastic deformation and the aerodynamic forces as a linked system.

1.2.2 Flow Separation and Reattachment Analysis

Although flow separation is essentially a fluid dynamics problem, the structural dynamics of the aerofoil may need to be taken into account if the aerofoil experiences significant deformation during the separation or reattachment process (as in the case of particularly flexible wings, for example). If the deformation substantially changes the flow properties, feedback loops, or forces acting on the structure, this turns into an elastodynamic issue.

Particularly in applications like morphing wings or flapping wing designs, structural deformations may affect flow separation and reattachment if the aerofoil is sufficiently flexible or experiencing significant deflections. The fluid-structure interaction needs to be dynamically taken into account in these situations.

1.2.3 Unsteady Aerodynamics

To effectively forecast the unstable response in time-dependent flow scenarios (e.g., when the aerofoil is in motion, such as in an oscillating or pitching aerofoil), the structural deformation and aerodynamic forces must be connected. For instance, aerodynamic forces

may cause an oscillating aerofoil to flex elastically, changing the flow dynamics.

The ensuing fluid-structure interaction turns into an elastodynamic issue if the aerofoil is elastic or if the deformation is substantial. It is a coupled fluid-structure problem that is elastodynamic in nature because of the way the aerofoil's dynamic motion (such as pitching or diving) interacts with the flow, producing time-dependent forces that are both structural and simply aerodynamic.

1.2.4 Aerofoil Shape Optimization

The deformation of the aerofoil may also need to be taken into account in optimization situations where the aerofoil is intended to meet particular performance goals (such as lift-to-drag ratio). Since aerofoils are often flexible in real-world applications, it is necessary to take into consideration the elastic deformations of the structure under aerodynamic loads in order to optimize the shape.

The flexible wings or adaptive aerofoils are being optimized for performance under different flow conditions. Structural dynamics would need to be coupled with fluid dynamics to accurately predict the performance of the aerofoil and optimize its shape.

In all of these cases, the structure (aerofoil) undergoes deformation in response to the aerodynamic forces, and this deformation feeds back into the fluid flow, making these elastodynamic problems. The Navier-Stokes equations for the fluid and the equations of motion for the elastic structure must be solved simultaneously in order to solve them using a coupled fluid-structure interaction (FSI) approach.

1.3 Fluid-Structure Interactions

Fluid-Structure Interactions happens when a flexible or rigid body with flexural support comes into touch with a fluid flow, which causes the structure to move [3]. Figure 1.1 depicts the system of interactions between fluid and solid structures. The fluid's velocity drops to zero at the stagnation point, which is the initial point of contact between the fluid and the structure. When compared to a free stream, the fluid flow behavior changes as a result of the solid body's movement. Flow-induced vibration is the movement of a solid structure brought on by fluid flow. Flow-induced vibration is the movement of a solid structure brought on by fluid flow. Vortex shedding, often referred to as "Von Kármán Vortex Street," is a phenomenon that happens when the fluid passes the bluff body and causes the vortices to alternately shed on the top and bottom sides of the structure. Figure 1.2 shows the classification of flow-induced vibration.

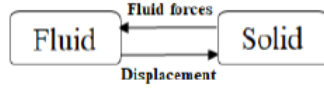


Figure 1.1: Fluid-structure interaction system

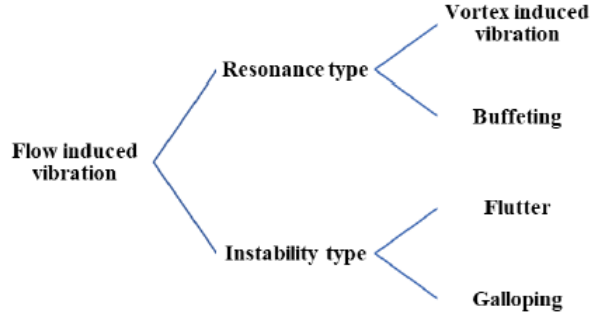


Figure 1.2: Classification fluid-induced vibration [1]

A dimensionless number is used to assess the oscillating flow called Strouhal number, which is defined as the ratio of inertial forces caused by local acceleration to that of convective acceleration. The equation for the Stokes number is given by:

$$St = \frac{f_s D}{U}$$

where St , f_s , D and U are Strouhal number, shedding frequency, diameter and flow velocity respectively.

1.4 Numerical Techniques

Numerical techniques involves the method of estimating an approximate solution to differential equation. It is crucial for modeling fluid flow issues that don't have an analytical answer. For a variety of uses, it has proven to be an accurate and affordable approach. These methods have the advantage of being able to design and optimize engineering systems, handle complex geometries, capture fluid flow variation in a time-dependent problem, analyze turbulent effects in a flow, and study flow characteristics when a fluid is subjected to internal or external forces, or both.

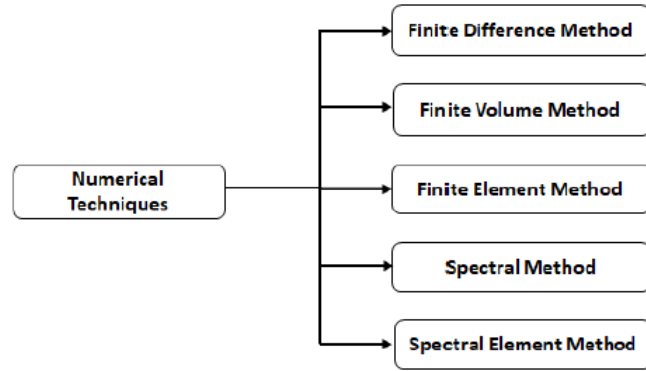


Figure 1.3: Mesh based numerical techniques to solve partial differential equation [2]

Figure 1.3 lists a few popular mesh-based numerical techniques for resolving partial differential equations. The problem’s complexity, the required level of precision, and the available computing power all influence the approach selection. Since every approach has pros and cons of its own, the problem statement must be taken into consideration when choosing the best approach.

1.4.1 Finite Difference Method

The Finite Difference Method (FDM) is a numerical technique used to solve differential equations by approximating derivatives with finite differences. This approach replaces the differential equations with difference equations that approximate the derivatives at discrete points by discretizing continuous variables, such time or space, into a grid. FDM is frequently used to model physical events in domains such as heat transfer, fluid dynamics, and structural analysis. Its benefits include simplicity and ease of use, which makes it appropriate for complex geometries. Its drawbacks include the requirement for fine grids to guarantee accuracy, which might raise computing expenses, and its potential inability to handle abrupt gradients or discontinuities.

1.4.2 Finite Volume Method

The Finite Volume Method (FVM) is a numerical technique used to solve partial differential equations, particularly in fluid dynamics and heat transfer, by dividing the domain into small, control volumes. The fluxes of conserved quantities (such as mass, momentum, and energy) are calculated across the borders of each control volume using this method, which integrates the governing equations across each control volume. The FVM is highly suited for imitating conservation rules because of its reputation for local quantity conservation. It is frequently applied to difficult flow behavior problems in computational fluid dynamics (CFD). FVM can be computationally demanding, particularly for high-resolution grids, and may necessitate careful handling of boundary conditions and dis-

cretization techniques in order to preserve accuracy, despite its robustness and guarantee of conservation of physical quantities.

1.4.3 Finite Element Method

The Finite Element Method (FEM) is numerical technique used to solve complex problems in engineering and physics, particularly for structural analysis, heat transfer, and fluid dynamics. The domain in FEM is separated into smaller, more straightforward sub-domains known as elements, which are often tetrahedrons in 3D or triangles or quadrilaterals in 2D. After discretizing the governing differential equations over these elements, the solution is shown as a collection of shape functions that characterize the behavior within each element. FEM is a strong tool for solid mechanics and multiphysics modeling problems because of its great flexibility and ability to handle complex geometries and boundary conditions. However, the accuracy is dependent on the mesh density, element selection, and numerical integration techniques, and it can be computationally costly, particularly for big problems with fine meshes. Figure 1.4 shows the fundamental framework for applying the finite element approach to solve a problem.

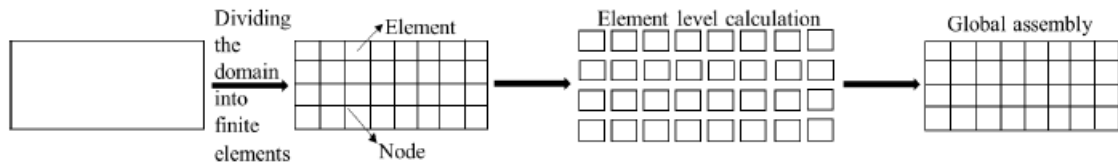


Figure 1.4: Basics of FEM

1.4.4 Spectral Method

In order to satisfy the differential equation, the concept underlying spectral methods is to express the solution as a summation of basis functions with adjustable coefficients specified in a continuous domain [4]. The Spectral Method connects the variables worldwide, as opposed to locally, as FEM does. In FEM, the basis functions are non-zero only on subdomains, but in general, they are non-zero over the entire domain. High accuracy and efficiency can result from this method, particularly for problems with periodic or nearly periodic behavior and smooth solutions. The total efficacy of the spectral technique for a given problem depends on the selection of basis functions, collocation locations, and problem-specific factors.

1.4.5 Spectral Element Method

The Spectral Element Method (SEM) is a variation of the Finite Element Method where a higher order basis function is used to obtain solution to the partial differential equation. Like the Spectral Methods, it offers precise approximations using a global basis function

and is adaptable and capable of handling complex geometries. Like FEM, the domain is separated into non-overlapping elements, and the solution is represented by higher order polynomials or spectral basis functions. To increase accuracy, orthogonal basis functions are selected for SEM.

While the finite element method is slower than spectral methods, it can handle complex geometries because it splits the computational domain into small and simple elements. In contrast, the spectral methods are superior in terms of computational time (using discrete Fourier transform, the number of operations reduces to $n\log(n)$) for a given accuracy when compared to other methods. However, because it incorporates the benefits of both spectral and finite element methods, the spectral element method has been chosen for this study because it has been shown to be a helpful strategy for discretizing a given set of governing equations.

1.5 Literature review

1.5.1 Development of SEM

The spectral element method was developed by Anthony T. Patera in 1984, where this technique was implemented to demonstrate a one-dimensional inflow-outflow advection diffusion equation and a two-dimensional flow in a channel expansion [5]. Patera demonstrates the effectiveness of the Spectral Element Method (SEM) by applying it to laminar flow in a channel expansion, showing significant improvements in accuracy over lower-order methods, particularly in capturing sharp velocity gradients near walls and regions of vortex formation. The SEM excels at resolving complex flow features, such as boundary layers and recirculating regions, with high precision and lower computational cost due to the spectral method's exponential convergence rate. Additionally, the method's flexibility in handling complex geometries with unstructured grids provides an advantage over traditional finite element methods, which typically rely on structured meshes.

1.5.2 Spectral element method

Using spectral elements has the advantage of being applicable in a variety of contexts, yielding consistent computational solutions and excellent accuracy for SFEM applications. The spectrum methods for highly nonlinear problems that the authors in [6] developed over a long period of time starting in 1969 include pseudo-spectral methods. Either collocation or a Galerkin methodology are commonly used to implement the spectrum approach. The spectral technique is special because it provides a workable substitute for series solutions for differential equations by enabling the symbolic description of solutions to small issues. Spectral approaches may be less expensive and easier to compute than finite element methods. They function well in simple issues with simple solutions when

high precision is needed. The global nature of step computation, however, makes the matrices involved dense, and applications will see a rapid decline in computational speed as the number of degrees of freedom increases.

1.5.3 Chebyshev spectral element method

The Gauss quadrature is typically used to estimate the mass matrix in the Chebyshev spectral element method (CSEM), which builds Lagrangian basis functions on the Gauss-Lobatto-Chebyshev (GLC) points. Thus, the CSEM, which is usually nondiagonal, is used to create the consistent mass matrix (CMM). The Chebyshev version was utilized in the earliest SEM works, but because the nondiagonal form mass matrix is computationally costly, it has not been widely applied for a variety of large-scale dynamic issues.

Wang *et al.* [7] developed a lumped mass Chebyshev spectral element method for solving structural dynamic problems. To employ the nodal quadrature method for mass lumping in CSEM, it is deduced that the Gauss-Lobatto-type quadrature, based on the Gauss-Lobatto-Chebyshev points with weighting function equal to unity. With the aid of this quadrature scheme, a lumped mass CSEM is constructed with a solid mathematical foundation. Based on the derived quadrature scheme, several 1-D and 2-D structural elements are designed to solve problems concerning eigenvalue or transient analysis in structural dynamics. For natural vibration problems, in most cases the lumped-mass CSEM can behave as well as traditional consistent-mass CSEM. In addition, it exhibits much faster convergence than does classical FEM. For the simulation of elastic wave propagation in rod, beam and plate structures, the proposed method achieves satisfactory performance. Considering its high efficiency in conjunction with explicit time-marching schemes, the lumped-mass CSEM is thus more favorable than traditional consistent-mass CSEM for conducting large-scale dynamic analysis

Zhu *et al.* [8] studied the Chebyshev spectral element method coupled with the implicit Newmark time integral method to simulate acoustic field. The method was initially used on a numerical example. The numerical result in this instance is in agreement with the reference solution, and the impact of the time step and the Newmark factor on numerical accuracy is examined. The following results show that numerical precision will increase with decreasing timestep and Newmark factor. The numerical accuracy can be affected by the computational domain's division pattern, meaning that it can be enhanced when the gridnode end to bed is distributed uniformly over the computational domain. The aforesaid approach is used to numerically examine a solution to a two-dimensional wave equation with given initial conditions and Dirichlet boundary conditions. The findings validate the generated method's features and performances.

Wang *et al.* [9] created a precise Chebyshev spectral element technique that uses the local thermal non-equilibrium model to mimic natural convection in a porous cavity. The

cavity's left vertical wall is heated, its right side wall is cooled, and its two horizontal walls are adiabatic. The algorithm's great accuracy is confirmed by the validation test with an exact solution, and the numerical results for natural convection in a porous square cavity show excellent agreement with solutions that have been published. It was seen that CSEM produces more accurate results than FEM when the same number of grids are used. The numerical oscillation can be observed in both FEM and CSEM, due to the coarse mesh. However, the numerical results of CSEM are more close to the reference results.

1.5.4 Legendre spectral element method(LSEM)

In order to estimate the mass matrix, the LSEM uses the Gauss-Lobatto-Legendre (GLL) quadrature algorithm and builds Lagrangian basis functions on GLL quadrature points. The lumped mass matrix (LMM) is constructed by the LSEM using this process, which is basically the nodal quadrature lumping approach.

Lotfi and Alipanah [10] numerically solved linear Volterra integro-differential equations with boundary conditions using the spectral element method to generate a discrete representation of the problem. They interpolated using the Legendre polynomials. Additionally, the method's error analysis is taken into account. The results demonstrated that the algorithm is efficient for obtaining approximation solutions of linear Volterra integro-differential equations.

Abbaszadeh *et al.* [11] developed a Legendre spectral element method (LSEM) for solving the stochastic nonlinear system of advection–reaction–diffusion models. The used basis functions are based on a class of Legendre functions such that their mass and diffuse matrices are tridiagonal and diagonal, respectively. The temporal variable is discretized by a Crank–Nicolson finite-difference formulation. In the stochastic direction, a random variable W based on the Q-Wiener process is employed. the rate of convergence and the unconditional stability for the achieved semi-discrete formulation is checked. Then, the Legendre spectral element technique is used to obtain a full-discrete scheme. The main advantage of the proposed numerical procedure is that the derived mass and diffuse matrices have tri-diagonal and diagonal forms, respectively.

1.5.5 Spectral Element-Fourier Method

Combining the benefits of Fourier spectrum methods and spectral element methods (SEM), the spectral Element Fourier method is a hybrid computational methodology. Partial differential equations (PDEs) in domains with periodic boundary conditions in one or more directions are especially well-solved using this approach.

Using a hybrid spectral element-Fourier technique, **Karniadakis** [12] suggested a solution for incompressible flow inside curved domains. For complex geometries with turbulent flows that have just one homogeneous flow direction, the approach produced results that were appropriate. Fast Helmholtz solvers and skew-symmetric convective

operators were utilized to reduce errors, and effective iterative algorithms such as the multigrid method can be utilized. Simulations for transitional-turbulent flow over rough wall surfaces and grooved channels were carried out to show the method's adaptability. A semi-implicit technique that directly addressed the nonlinear convective term was used to present direct numerical simulation for grooved channels [13]. An technique that could simulate convection events in axisymmetric rotating containers was proposed by **Fournier *et al.*** [14]. For the non-periodic direction, they employed the Gauss-Lobatto-Jacobi quadrature in conjunction with a parallel spectral element approach. A second-order timestepping approach was used to implicitly treat the Coriolis and viscous forces. Analytical findings for spherical and cylindrical coordinates were contrasted with the numerical solution. The work suggests a unique Fourier-Legendre spectral element method for resolving Poisson-type equations in polar coordinates, which is based on the Galerkin formulation.

A three-dimensional spectral-element/Fourier smoothed profile approach (SEF-SPM) was created by **Wang *et al.*** [15] to model turbulent flows past moving bluff bodies. In the meshing process, a combination of triangular and quadrilateral elements were employed. Large eddy simulations were made possible by the introduction of the Entropy Viscosity Method (EVM). The technique was tested for turbulent flow past stationary and moving cylinders at Reynolds numbers between 80 and 10,000 as well as flow past a stationary sphere at Reynolds numbers between 200 and 1000. A self-excited, rigidly moving dual-step cylinder was simulated for the vortex-induced vibration case, demonstrating the method's effectiveness in problem analysis.

1.6 Objectives

- To develop a MATLAB-based code that implements the SEM for solving transient problems, ensuring efficient discretization of the governing equations and accurate approximation of the solution fields.
- To solve steady heat diffusion and unsteady heat diffusion problem using the developed code.
- To accurately capture and simulate the interaction between a fluid and a structure focusing on the coupling effects between the solid and fluid domains.

1.7 Structure of Thesis

The thesis is organized as follows, in the first chapter 1 a brief introduction to Spectral element method and Numerical techniques is given, the literature survey of mentioned topics is done and then the objectives of the current work are enumerated. In the second

chapter 2 the formulation and methodology to do spectral element method of a given domain and how weak form of governing differential equation can be derived. After that a two problems are solved by using both FEM and SEM. The results obtained are compared. The summary of entire work is given in 3.

Chapter 2

Methodology

2.1 Overview of SEM

The detailed formulation of the Spectral Element Method is represented in figure 2.1. The main difference between SEM and Spectral techniques is the use of higher order piecewise polynomials as the basis functions for faster convergence over the entire domain.

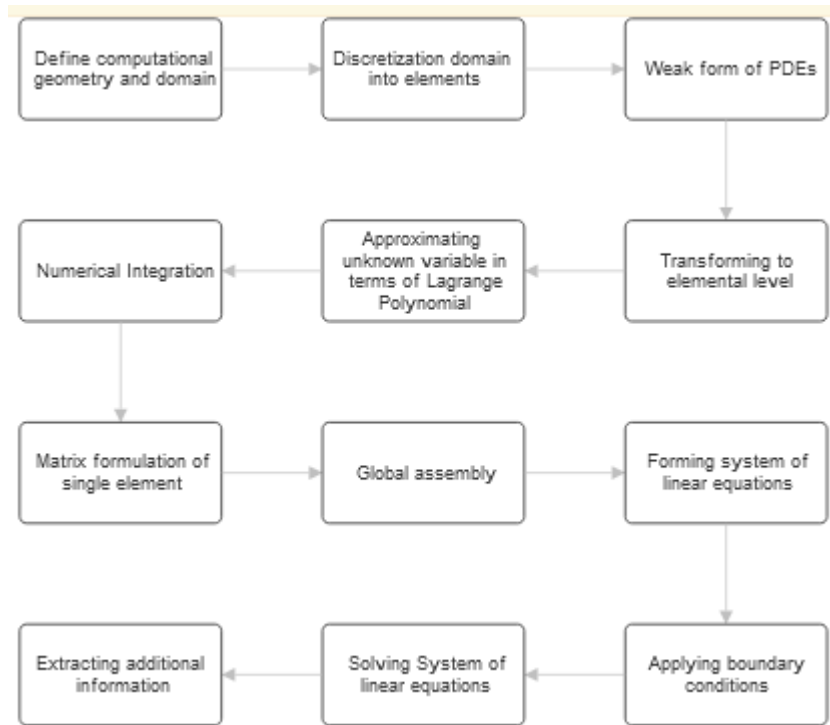


Figure 2.1: SEM flowchart

One-dimensional steady-state Heat conduction equation is chosen to explain the details of SEM. The equation is given as:

$$k \frac{d^2 f}{dx^2} + s(x) = 0 \quad (2.1)$$

$$q_0 \equiv -k \left(\frac{df}{dx} \right)_{x=0} \quad (2.2)$$

$$f(x = L) \equiv f_L \quad (2.3)$$

2.2 Galerkin Weak Formulation

The weak form a PDE is obtained by product of the original PDE with a set of basis functions and integrating it over the domain. Weak form ensures that the solution satisfies the PDE in an average sense rather than pointwise. The dependent variable and the source term are approximated using nodal expansion.

$$f(x) = \sum_{j=1}^{N_E+1} f_j \phi_j(x) \quad (2.4)$$

$$s(x) \simeq \sum_{j=1}^{N_E+1} s_j \phi_j(x) \quad (2.5)$$

substituting in the governing differential equation reduces to:

$$k \frac{d^2 f(x)}{dx^2} + s(x) = \epsilon \quad (2.6)$$

ϵ is the residual obtained from approximation.

$$s = s_N + \epsilon \quad (2.7)$$

$$s_N = \phi_0 s_0 + \phi_1 s_1 + \dots \quad (2.8)$$

Figure 2.2 implies that residual ϵ is minimum when s_N is perpendicular to ϵ .

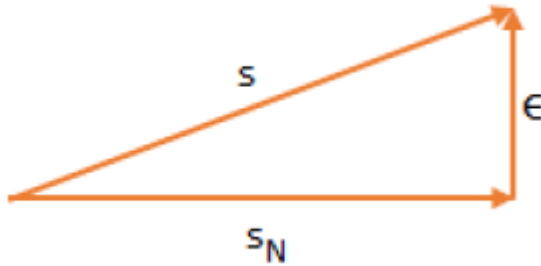


Figure 2.2: Body-aligned mesh for case that the Orthogonality of ϵ

$$0 = \int_{\Omega_e} s_N \epsilon d\Omega = s_0 \int_{\Omega_e} \phi_0 \epsilon d\Omega + s_1 \int_{\Omega_e} \phi_1 \epsilon d\Omega + \dots \quad (2.9)$$

In order to minimize the error, imposing orthogonality of ϕ_i and ϵ

$$\int_{\Omega_e} \phi_i \epsilon d\Omega = 0 \quad \text{where} \quad i = 0, 1, 2, \dots, N \quad (2.10)$$

Substituting ϵ in the above equation, we have

$$\int_0^L \phi_i(x) \left(k \frac{d^2 f}{dx^2} + s(x) \right) dx = 0 \quad (2.11)$$

Integrating by parts,

$$\int_0^L \left(k \frac{d}{dx} \left(\phi_i \frac{df}{dx} \right) - k \frac{d\phi_i}{dx} \frac{df}{dx} + \phi_i s(x) \right) dx = 0 \quad (2.12)$$

Implementing Neumann boundary condition,

$$\delta_{i,1} q_0 - k \int_0^L \frac{d\phi_i}{dx} \frac{df}{dx} dx + \int_0^L \phi_i s(x) dx = 0 \quad (2.13)$$

2.3 Formulation of linear algebraic system

Substituting equation 2.4 and 2.5 in equation 2.15

$$\sum_{j=1}^{N_E} \left(\int_0^L \frac{d\phi_i}{dx} \frac{d\phi_j}{dx} dx \right) f_j = - \left(\int_0^L \frac{d\phi_i}{dx} \frac{d\phi_{N+1}}{dx} dx \right) f_L + q_0/k \delta_{i,1} + \frac{1}{k} \sum_{j=1}^{N_E+1} \left(\int_0^L \phi_i \phi_j dx \right) s_j \quad (2.14)$$

The Dirichlet boundary condition has been specified at $x=L$, transferring the terms multiplying the corresponding value, f_L we derive a linear system,

$$\mathbf{D} \cdot \mathbf{f} = \mathbf{b} \quad (2.15)$$

where \mathbf{f} is the vector of unknown temperatures at the nodes,

$$\mathbf{f} \equiv [f_1, f_2, \dots, f_{N_E-1}, f_{N_E}]^T \quad (2.16)$$

where \mathbf{D} is the $N_E \times N_E$ global diffusion matrix.

$$\mathbf{b} \equiv \mathbf{c} + \frac{1}{k} \mathbf{M} \cdot \mathbf{s} \quad (2.17)$$

where \mathbf{c} encapsulates the boundary conditions,

$$\mathbf{c} \equiv [q_0/k, 0, \dots, 0, f_L/h_{N_E}]^T \quad (2.18)$$

where \mathbf{s} contains nodal values at the source,

$$\mathbf{s} \equiv [s_1, s_2, \dots, s_{N_E}, s_{N_E+1}]^T \quad (2.19)$$

2.4 Element Level Transformation

Element level transformation refers to the process of mapping the reference element in the computational to physical element, so that calculations can be performed in the local coordinate system of each element. It helps to accurately represent a complex domain geometry and achieve high order accuracy. Transformation of physical domain into computational domain in 1D is represented in figure 2.3

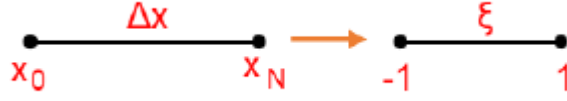


Figure 2.3: Transformation in 1D

$$x = \frac{(x_0 + x_N)}{2} + \frac{(x_N - x_0)}{2} \xi \quad (2.20)$$

x-coordinate:

$$\xi = \frac{2(x - x_0)}{\Delta x^e} - 1 \quad (2.21)$$

Jacobian:

$$|J| = \frac{\partial x}{\partial \xi} = \frac{\Delta x^e}{2} \quad (2.22)$$

$$\frac{\partial \psi(x)}{\partial x} = \frac{\partial \psi(\xi)}{\partial \xi} \frac{\partial \xi(x)}{\partial x} = \frac{\partial \psi(\xi)}{\partial \xi} \frac{2}{\Delta x^e} \quad (2.23)$$

Mass matrix:

$$\mathbf{M}_{ij} = \int_{X_1^l}^{X_2^l} \phi_i(x) \phi_j(x) dx = \frac{1}{2} \Delta x \int_{-1}^1 \phi_i(\xi) \phi_j(\xi) d\xi \quad (2.24)$$

Diffusion Matrix:

$$\mathbf{D}_{ij} = \int_{\mathbf{x}_1^l}^{\mathbf{x}_2^l} \frac{d\phi_i(\mathbf{x})}{d\mathbf{x}} \frac{d\phi_j(\mathbf{x})}{d\mathbf{x}} d\mathbf{x} = \frac{2}{\Delta \mathbf{x}} \int_{-1}^1 \frac{d\phi_i(\xi)}{d\mathbf{x}} \frac{d\phi_j(\xi)}{d\mathbf{x}} d\xi \quad (2.25)$$

2.5 Interpolation

Approximating a function $f(x)$ by an interpolant of degree N (I_N) is called interpolation.

$$I_N(f(x_i)) = f(x_i) \quad (2.26)$$

2.5.1 Nodal Interpolation

Nodal interpolation directly interpolates the value of function at specific points inside the element and uses these values to approximate the function using polynomial basis function.

$$f(x) = \sum_{j=0}^N L_j(x) f_j \quad (2.27)$$

where L denotes Lagrange polynomial.

2.5.2 Lagrange Polynomials

The expression for Lagrange polynomial is given by

$$L_i(x) = \prod_{\substack{j=0 \\ j \neq i}}^N \frac{x - x_j}{x_i - x_j} \quad (2.28)$$

Assuming ϕ_N to be the generating polynomial

$$\phi_N(x) = \prod_{j=0}^N (x - x_j) \quad (2.29)$$

The derivative of generating polynomial is

$$\phi'_N(x) = \sum_{k=0}^N \frac{1}{(x - x_k)} \prod_{j=0}^N (x - x_j) \quad (2.30)$$

for $x = x_i$, yields

$$\phi'_N(x_i) = \prod_{\substack{j=0 \\ j \neq i}}^N (x_i - x_j) \quad (2.31)$$

$$L_i(x) = \frac{\phi_N(x)}{\phi'_N(x_i)(x - x_i)} \equiv \prod_{\substack{j=0 \\ j \neq i}}^N \frac{x - x_j}{x_i - x_j} \quad (2.32)$$

Above equation gives the relationship between generating polynomials and Lagrange basis functions. There is a requirement to know the derivative of the Lagrange polynomials.

$$\frac{dL_i}{dx}(x) = \sum_{\substack{k=0 \\ k \neq i}}^N \left(\frac{1}{x_i - x_k} \right) \prod_{\substack{j=0 \\ j \neq i \\ j \neq k}}^N \frac{x - x_j}{x_i - x_j} \quad (2.33)$$

2.5.3 Lobatto polynomials

The Lobatto polynomials are obtained using the Legendre polynomials as follows

$$\varphi_{\text{Lob}}^N(x) = (1+x)(1-x) \frac{d}{dx} \varphi_{\text{Leg}}^{N-1}(x) \quad \varphi_{\text{Lob}}^N(x) \equiv (1-x^2) \frac{d}{dx} \varphi_{\text{Leg}}^{N-1}(x) \quad \forall N \geq 2 \quad (2.34)$$

Legendre and Lobatto polynomials and the roots and weights of Lobatto polynomials for different order of polynomials are shown in fig. 2.4 and 2.5.

Order of Polynomial	Legendre Polynomial	Lobatto Polynomial
1	x	-
2	$\frac{1}{2}(3x^2 - 1)$	$(1 - x^2)$
3	$\frac{1}{2}(5x^3 - 3x)$	$3x(1 - x^2)$
4	$\frac{1}{8}(35x^4 - 30x^2 + 3)$	$\frac{1}{2}(15x^2 - 3)(1 - x^2)$

Figure 2.4: Legendre and Lobatto polynomial

Order of Polynomial	Roots					Weights				
2	-1	+1				1	1			
3	-1	0	+1			1/3	4/3	1/3		
4	-1	-0.447214	+0.447214	+1		5/3	5/6	5/6	5/3	
5	-1	-0.654654	0	0.654654	+1	1/10	49/90	32/45	49/90	1/10

Figure 2.5: Lobatto roots and weights

The node locations for polynomial order 1 to 7 is represented in 2.6 .It is quite clear that the Chebyshev points and Lobatto points are well behaved while estimating the Lagrange polynomial, whereas, equi-spaced points show huge oscillations near the end points while interpolating a functions. The comparison between the interpolation of Runge's function by equispaced interpolation point, Chebyshev points and lobatto points is presented in figure 2.7.

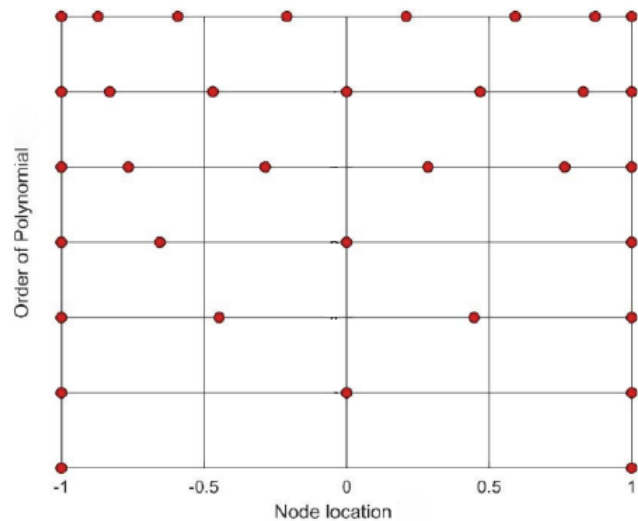
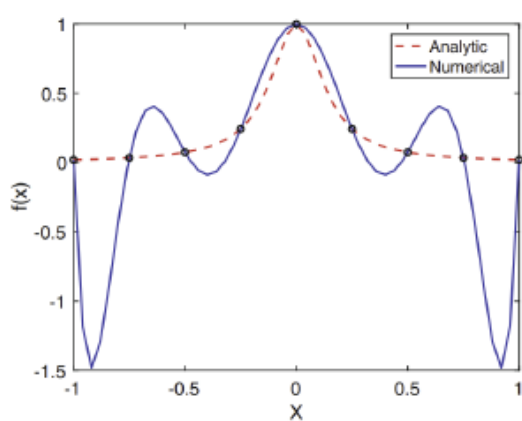
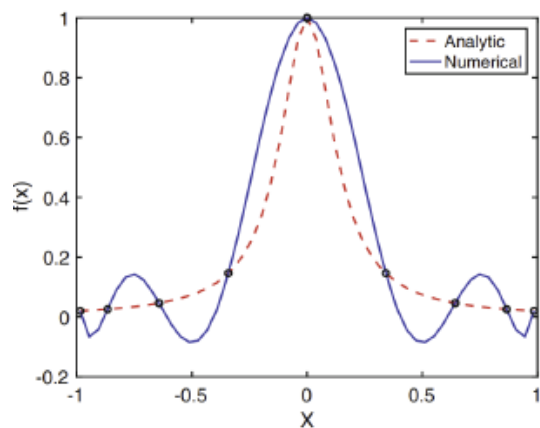


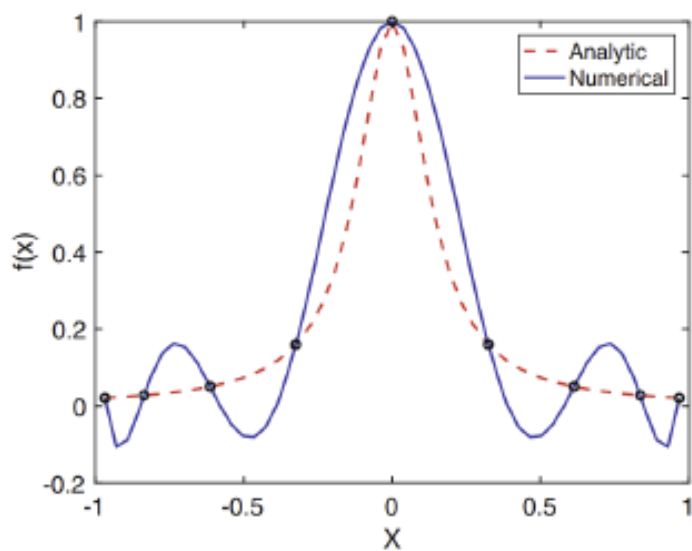
Figure 2.6: Node location for Lobatto points



(a) Equi-spaced interpolation points



(b) Chebyshev points



(c) Lobatto points

Figure 2.7: Interpolation of Runge's function

2.6 Steady Heat Diffusion in One Dimension

The steady heat diffusion problem, describes the distribution of temperature within a medium under steady-state conditions, where the temperature field does not change with time. In this scenario, heat flow is governed by Fourier's law of heat conduction, and the temperature distribution is determined by the balance between heat entering and exiting a material. The conservation of energy yields the governing equation for steady-state heat diffusion. Solving the steady heat diffusion problem is crucial in various engineering and scientific applications, including heat exchanger design, thermal analysis of structures, and materials science. Predicting temperature gradients and maximizing thermal performance require precise solutions.

The objective of this problem is to numerically solve the steady-state heat diffusion equation for a one-dimensional domain with the following given parameters:

Domain length: $L = 1.0$

Thermal conductivity: $k = 1.0$

Heat source: $q_0 = 1.0$

Boundary condition at $x=L$: $f(L) = 0.0$

A specific source term: $s_0 = 10$

Consider heat conduction through a circular rod of length L at steady state, in the presence of a distributed heat source as illustrated in figure 2.12

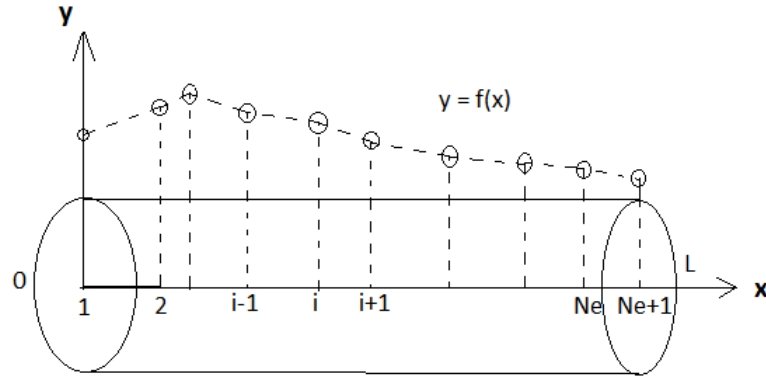


Figure 2.8: Conduction through a rod extending from $x=0$ to $x=L$ at steady state.

The governing differential equation for the problem is

$$k \frac{d^2 f}{dx^2} + s(x) = 0 \quad (2.35)$$

where $s(x)$ is the rate of heat production

Boundary conditions

(a) the heat flux at the left end of the rod located at $x=0$

$$q_0 \equiv -k \left(\frac{df}{dx} \right)_{x=0} \quad (2.36)$$

(b) Temperature at right end of the rod at $x=L$

$$f(x = L) = f_L \quad (2.37)$$

where f_L is a constant.

Finite element interpolation

The domain is divided into N_E intervals determined by element end nodes located at positions x_i for $i=1, \dots, N_E+1$ where $x_1 = 0$ and $x_{N_E+1} = L$. The temperature distribution is approximated over the individual elements with linear functions whose union yields a continuous, piecewise linear function. This would be sufficient since the order of the differential equation in the weak form is one. Element grading is done to ensure spatial resolution by varying the element size manually. By keeping the ratio as one the elements are of equal size.

To generate the coefficient matrix and right hand side of linear system, global integration formulas are used. While implementation these integrals need to be assembled in a systematic way. This is done with the help of connectivity matrix which maps local element nodes to global nodes. The tridiagonal nature of the global diffusion matrix \mathbf{D} allows us to solve the linear system using Thomas algorithm.

2.6.1 Results

The solution is generated for gaussian source function

$$s(x) = s_0 \exp(-5x^2/L^2) \quad (2.38)$$

Calculations for a specified value of element stretch ratio $\text{ratio}=5$ and number of elements varied ,

$$N_E = 8, 16, 32, 64, 128, 256 \quad (2.39)$$

yield left end value

$$f(0) = 1.9746, 1.9662, 1.9644, 1.9640, 1.9639, 1.9639 \quad (2.40)$$

and for uniformly spaced elements, $\text{ratio} = 1$

$$f(0) = 1.9510, 1.9606, 1.9631, 1.9637, 1.9638, 1.9639 \quad (2.41)$$

These results clearly indicate that $f(0) = 1.9639$ is the exact solution, the numerical error $e(0) = f(0) - 1.9639$

$$e(0) = -0.0129 - 0.0032 - 0.0008 - 0.0002 - 0.00010.0000 \quad (2.42)$$

These numerical results suggest that when the number of elements is doubled, the numerical error decreases approximately by a factor of 4. The error is proportional to h^2 .

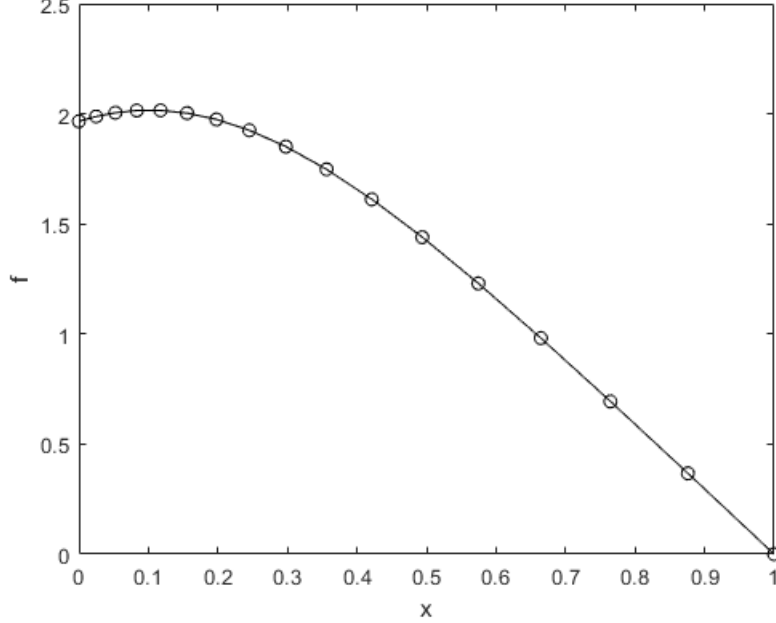


Figure 2.9: Finite element solution of steady diffusion equation with 16 linear elements with parameters $L=1.0, k=1.0, q_0=-1.0, f(L)=0.0, s_0=10.0$

In spectral element method, the element interpolation nodes are distributed at the zeros of appropriate family of orthogonal polynomials over the canonical interval of the ξ axis subject to the mandatory constraints that the first node is placed at $\xi=-1$ and last node $\xi_{m+1}=1$, where m is the order of the polynomial expansion defined by $m+1$ nodes. The function `discr lob` defines the element end points and generates lobatto interpolation nodes and returns the global nodes and connectivity matrix. The extra last column and row of the global diffusion matrix as well as entry of right hand side vector is removed (Dirichlet BC). The solution is generated by the code for the Gaussian source function. To assess whether implementing the higher order method is worthy of the additional analytical and programming effort, we compare the spectral element solution with the solution of finite element method that employs linear elements. Properly scaled values of the solution at the left end $f(x=0)$, computed with (a) the consistent spectral element method (b) the mass lumped spectral element method and (c) The finite element method. With element spaced evenly in all cases.

Spectral N_G	N_E	N_P	consistent $f(0)$	Lumped $f(0)$	Linear uniform	$f(0)$
3	2	1	1.8024	2.2163	2	1.8024
5	2	2	1.9512	1.9512	4	1.9140
7	2	3	1.9643	1.9643	6	1.9412
9	2	1	1.9638	1.9638	8	1.9510
11	2	1	1.9639	1.9639	10	1.9556
16	2	1	1.9639	1.9639	15	1.9602
					32	1.9632
					64	1.9637
					128	1.9638

Table 2.1: Accuracy and convergence of the spectral element method compared to the finite element method.

The results reveal that the effect of mass lumping is insignificant for all but the crudest discretization. Comparison of the numerical solutions for a fixed number of global nodes, N_G clearly demonstrates the superiority of the spectral element method over the finite element method. For example, the spectral element solution with 16 global nodes, $N_G=16$, is accurate to the fifth significant figure, whereas the finite element solution with 128 global nodes, $N_G=128$, is accurate only to the fourth significant figure.

Accuracy The performance of the spectral element method can be quantified further with reference to the steady diffusion equation in the interval $[0,L]$ with source term

$$s(x) = -s_0 \exp(x/L) \quad (2.43)$$

where s_0 is a constant. The relative error at the left end value defined as

$$E \equiv |f(0)/f_0 - 1.0| \quad (2.44)$$

Relative error is plotted against available degree of freedom, N , on a log-log scale. In case of FEM, N is the no. of evenly spaced elements, N_E . In case of spectral element method, N is the expansion of the one element solution, $N_E=1$.

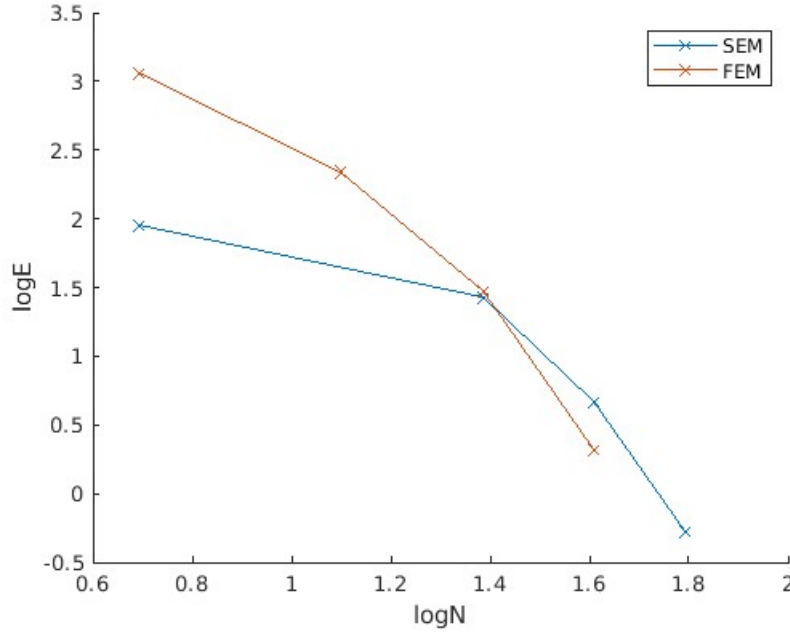


Figure 2.10: Error for left end value for the model problem.

As the polynomial degree increases, the error in the spectral element method increases at a faster rate than finite element method.

Runge function

Runge function is a rational function, and is often used to demonstrate the behavior of polynomial interpolation at equispaced nodes.

In a more stringent test, we consider steady diffusion equation in the presence of the source term

$$s(x) = 200s_0 \frac{1 - 75x^2}{(1 + 25x^2)^3} \quad (2.45)$$

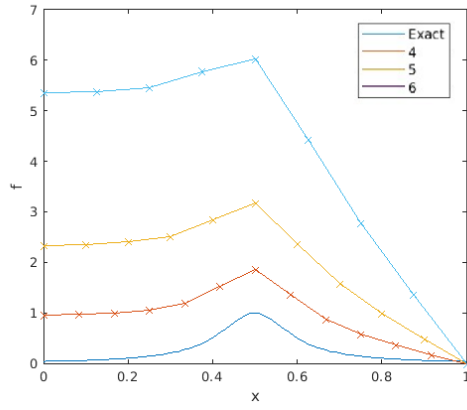
with the exact solution being

$$f(x) = \frac{s_0 L^2}{k(1 + 25x^2)} \quad (2.46)$$

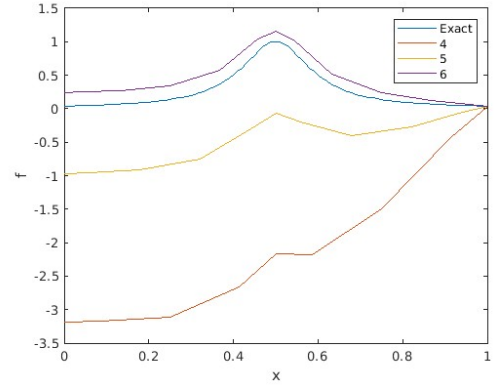
Numerical solutions with two elements of equal size, $N_E=2$, and an increasing number of (a) even spaced or (b) spectral nodes. The exact solution is represented by smooth line in both graphs. The numerical solution with evenly spaced nodes suffer from oscillations, exhibiting an apparent lack of convergence as the polynomial order increases from lower values. The numerical solution with spectral node exhibit a uniform improvement showing a better behaviour.

2.7 Unsteady Heat Diffusion in One Dimension

The unsteady heat diffusion problem, also known as the transient heat conduction problem, involves the time-dependent distribution of temperature within a medium where heat



(a) Even spaced finite elements



(b) Spectral nodes

transfer occurs both spatially and temporally. Unlike the steady-state case, the temperature in an unsteady heat diffusion problem varies with time, requiring the solution of the heat conduction equation that accounts for both the spatial and temporal changes in temperature. Unsteady heat diffusion is prevalent in various engineering and scientific applications, such as thermal analysis of transient processes in materials, cooling or heating of structures, and heat storage systems. Solving this problem accurately is crucial for predicting temperature variations over time and understanding dynamic thermal behaviors.

Consider the unsteady version of the heat conduction problem in the presence of a distributed source.

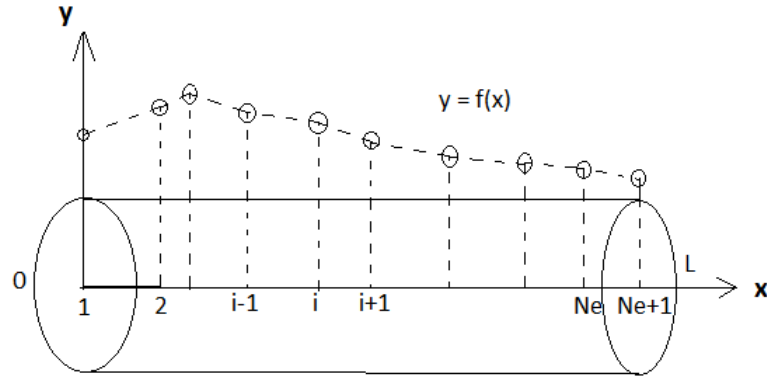


Figure 2.12: Conduction through a rod extending from $x = 0$ to $x = L$ at steady state.

The governing differential equation for the problem is given by

$$\frac{\partial f}{\partial t} = \kappa \frac{\partial^2 f}{\partial x^2} + \frac{s(x, t)}{\rho c_p} \quad (2.47)$$

where

$$\kappa \equiv \frac{k}{\rho c_p} \quad (2.48)$$

is the thermal diffusivity. Subject to given initial condition $f(x, t = 0) = F(x)$ and two boundary conditions, one at each end.

The objective of this problem is to numerically solve the unsteady heat diffusion equation for a one-dimensional domain with the following given parameters:

Domain length: $L = 1.0$

Density: $\rho = 1.0$

Specific heat capacity: $c_p = 1.0$

Thermal conductivity: $k = 1.0$

Heat source: $q_0 = 1.0$

Time step: $\Delta t = 0.01$

Number of time steps: $n_{steps} = 100$

The goal is to numerically solve this unsteady heat diffusion problem using the Spectral Element Method (SEM), to compute the time-dependent temperature distribution $T(x, t)$ over the given domain, subject to the specified boundary, initial conditions, and other parameters.

2.7.1 Galerkin weak formulation

To formulate the weak form, we follow the steps outlined for steady diffusion. The main difference is the unknown nodal values $f_i(t) \equiv f(x_i, t)$ is now time dependent. The i th Galerkin projection yields

$$\rho c_p \int_0^L \phi_i \frac{\partial f}{\partial t} dx = -k \left(\phi_i \frac{\partial f}{\partial x} \right)_{x=0} + k \left(\phi_i \frac{\partial f}{\partial x} \right)_{x=L} - k \int_0^L \frac{\partial \phi_i}{\partial x} \frac{\partial f}{\partial x} dx + \int_0^L \phi_i s(x, t) dx \quad (2.49)$$

where i runs over an appropriate number of nodes determined by the degree of the element interpolation function and boundary conditions. Substituting expansion of numerical solution

$$\mathbf{f}(x, t) = \sum_{j=1}^{N_G} f_j(t) \phi_j(x) \quad (2.50)$$

and corresponding expansion for source term

$$\mathbf{s}(x, t) = \sum_{j=1}^{N_G} s_j(t) \phi_j(x) \quad (2.51)$$

where N_G is the number of unique global nodes.

Rearranging and collecting all nodal projections, we have a system of linear ordinary differential equations (ODEs),

$$\mathbf{M} \frac{d\mathbf{f}}{dx} + \kappa \mathbf{D} \cdot \mathbf{f} = \kappa \mathbf{b} \quad (2.52)$$

where \mathbf{M} is global mass matrix, \mathbf{D} is global diffusion matrix and \mathbf{b} is right hand side. To circumvent the restriction on the time step, an implicit method, Crank-Nicolson method is used. A time step Δt is selected and the differential equation is evaluated at $t + \frac{1}{2}\Delta t$ and approximate the time derivative on the left hand side with center finite difference and rest of the terms with averages to obtain

$$\mathbf{M} \frac{\mathbf{f}^{(n+1)} - \mathbf{f}^{(n)}}{\Delta t} + \frac{1}{2} \kappa \mathbf{D} (\mathbf{f}^{(n)} + \mathbf{f}^{(n+1)}) = \frac{1}{2} \kappa (\mathbf{b}^{(n)} + \mathbf{b}^{(n+1)}) \quad (2.53)$$

Rearranging, we derive a linear algebraic system,

$$\mathbf{C} \cdot \mathbf{f}^{(n+1)} = \mathbf{r} \quad (2.54)$$

where the coefficient matrix is given by

$$\mathbf{C} = \mathbf{M} + \frac{1}{2} \kappa \Delta t \mathbf{D} \quad (2.55)$$

and right hand side is given by

$$\mathbf{r} = \left(\mathbf{M} + \frac{1}{2} \kappa \Delta t \mathbf{D} \right) \cdot \mathbf{f}^{(n)} + \frac{1}{2} \kappa (\mathbf{b}^{(n)} + \mathbf{b}^{(n+1)}) \quad (2.56)$$

The numerical procedure involves solving the linear system from a initial state for a sequence of steps with a constant Δt . The solution at each step can be found efficiently using the Thomas algorithm.

The spectral element method is implemented in the following steps.

1. Define input and parameter definition.
2. Element and node definition.
3. Specification of initial temperature distribution and definition of the source distribution along the rod.
4. Computation of global diffusion and mass matrix by Lobatto quadrature.
5. Compilation of linear system, computation of coefficient matrix at each time step and evaluation of time independent \mathbf{b} outside time loop and updating in each time loop.
6. Solution of the linear system.
7. Plotting the transient solution.
8. Return to step 5 until termination of time steps.

2.7.2 Results

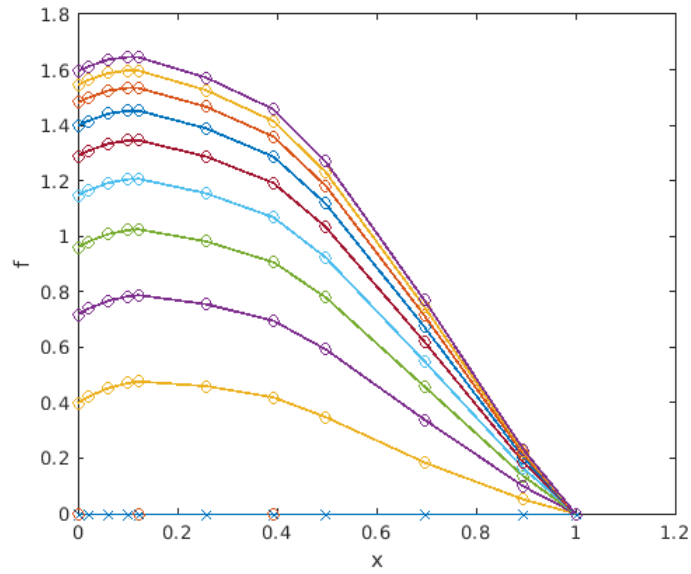


Figure 2.13: Solution to unsteady diffusion equation by implementing the Crank-Nicolson method

The solution generated by the code is displayed in figure 2.13 . The right end Dirichlet Boundary specified $fL=0$, the initial condition specifies that $f(x,t=0)=0$ and other parameters are $L=1.0$, $\rho=1.0$, $cp=1.0$, $k=1.0$, $q_0=-1$, $dt=0.01$, $nsteps=100$; As time progresses, the transient solution smoothly tends to the steady-state solution, in agreement with physical intuition.

Chapter 3

Summary

This report presents the development of a Spectral Element Method (SEM) in MATLAB for solving the 1-D heat diffusion problem in both steady-state and unsteady-state scenarios. The SEM, which combines the flexibility of element-based discretization with the advantages of high-order polynomial approximations from spectral approaches, is described in the study along with its formulation and implementation.

Under the presumption of unchanging thermal characteristics, the SEM solves the governing differential equation with boundary conditions to produce precise and effective solutions for the steady-state heat diffusion problem. The Crank-Nicolson approach is used to solve the transient heat diffusion equation in the unsteady-state scenario by extending the SEM to include time-dependent phenomena.

The Runge function, a widely used reference in the literature for heat diffusion problems, is used to compare the SEM results with known solutions. The comparisons show how accurate the SEM is, emphasizing how well it can depict the behavior of both steady and erratic heat diffusion.

Additionally, a comparison with the Finite Element Method (FEM), a popular numerical method for resolving differential equations, is carried out. SEM's capacity to describe the solution with fewer degrees of freedom makes it more accurate and computationally efficient than FEM, particularly for high-order approximations. The study also examines how the two approaches converge, demonstrating the SEM's higher rate of convergence. Overall, this report's results confirm that the Spectral Element Method is a viable substitute for more conventional approaches like FEM in 1-D heat diffusion issues, especially for applications that demand high accuracy and computing economy.

3.1 Future Work

Building upon the foundation of the Spectral Element Method (SEM) code developed for solving steady and unsteady heat diffusion problems, the focus will be on extending the methodology to address more complex fluid dynamics problems, specifically the Navier-Stokes equations. The extension of the current SEM solver to the Navier-Stokes framework will provide a robust numerical tool for the analysis of fluid flows in conjunction with the deformation of structures, which is essential for understanding aerodynamics, heat transfer, and vibration interactions in aerofoil design and optimization.

References

- [1] M. Armandei, A. C. Fernandes, and A. B. Rostami. Hydroelastic buffeting assessment over a vertically hinged flat plate. *Experimental Techniques*, 40:833–839, 2016.
- [2] M. B. Hafeez and M. Krawczuk. A review: Applications of the spectral finite element method. *Archives of Computational Methods in Engineering*, 30(5):3453–3465, 2023.
- [3] Y. Modarres-Sadeghi. *Introduction to Fluid-Structure Interactions*. Springer Nature, 2022.
- [4] C. Canuto. *Spectral Methods: Evolution to Complex Geometries and Applications to Fluid Dynamics*. Springer-Verlag, 2007.
- [5] A. T. Patera. A spectral element method for fluid dynamics: laminar flow in a channel expansion. *Journal of computational Physics*, 54(3):468–488, 1984.
- [6] W. H. Press. *Numerical recipes in Fortran 90: Volume 2, volume 2 of Fortran numerical recipes: The art of parallel scientific computing*, volume 2. Cambridge university press, 1996.
- [7] J. Wang, H. Li, and H. Xing. A lumped mass chebyshev spectral element method and its application to structural dynamic problems. *Earthquake Engineering and Engineering Vibration*, 21(3):843–859, 2022.
- [8] C. Zhu, G. Qin, and J. Zhang. Implicit chebyshev spectral element method for acoustics wave equations. *Finite elements in analysis and design*, 47(2):184–194, 2011.
- [9] Y. Wang, G. Qin, W. He, and Z. Bao. Chebyshev spectral element method for natural convection in a porous cavity under local thermal non-equilibrium model. *International Journal of Heat and Mass Transfer*, 121:1055–1072, 2018.
- [10] M. Lotfi and A. Alipanah. Legendre spectral element method for solving volterra-integro differential equations. *Results in Applied Mathematics*, 7:100116, 2020.
- [11] M. Abbaszadeh, M. Dehghan, A. Khodadadian, and T. Wick. Legendre spectral element method (lsem) to simulate the two-dimensional system of nonlinear stochastic advection–reaction–diffusion models. *Applicable Analysis*, 101(6):2279–2294, 2022.

- [12] G. Karniadakis. Spectral element-fourier methods for incompressible turbulent flows. *Computer Methods in Applied Mechanics and Engineering*, 80(1-3):367–380, 1990.
- [13] C. H. Amon. Spectra element-fourier method for transitional flows in complex geometries. *AIAA journal*, 31(1):42–48, 1993.
- [14] A. Fournier, H.-P. Bunge, R. Hollerbach, and J.-P. Vilotte. A fourier-spectral element algorithm for thermal convection in rotating axisymmetric containers. *Journal of Computational Physics*, 204(2):462–489, 2005.
- [15] Z. Wang, M. S. Triantafyllou, Y. Constantinides, and G. E. Karniadakis. A spectral-element/fourier smoothed profile method for large-eddy simulations of complex viv problems. *Computers & Fluids*, 172:84–96, 2018.